Transition states, electronic structure, and magnetic properties of small-sized nickel clusters

Omar López-Estrada and Emilio Orgaz

Departamento de Física y Química Teórica, Facultad de Química, Universidad Nacional Autónoma de México, Cd. Universitaria, CP 04510, México, Mexico

(Received 11 November 2014; revised manuscript received 5 February 2015; published 26 February 2015)

Density functional computations of the electronic structure of small-sized nickel clusters (Ni_n, $2 \leqslant n \leqslant 12$) have been carried out. We explored the potential energy surface at different spin multiplicities starting from guess structures obtained by statistical sampling. We focus this work on the search of the ground-state geometries and their magnetic properties. In some cases, close in energy geometries appear allowing a competition for the ground-state structure. For such cases, we investigated the energy profiles by searching for the transition states that connect structures belonging to different spin multiplicities.

DOI: 10.1103/PhysRevB.91.075428 PACS number(s): 63.22.Kn, 73.22.Pr, 75.75.Lf

I. INTRODUCTION

During the last decade, nickel nanoparticles have been investigated owing to their potential as well as actual applications in catalysis [1–3] and magnetism [4,5]. The fundamental properties of small-sized nickel aggregates are still a subject of controversy [6–10], in particular, their ground-state structures and, in some cases, their magnetism, as in Ni_5 [6,7,11] and Ni_7 [8,9] clusters. It is important to mention that for some small-sized Ni clusters, the occurrence of noncollinear magnetism has been investigated before [11]. In several small-sized transition-metal clusters, this phenomenon slightly modifies the binding energies and geometries. However, the impact on the total and local magnetism is relevant in low-symmetry structures, in particular for transition metals with uncompleted d bands [12–17], and in $4d$, $5d$ [11], and $4f$ [18,19] metals. Spin frustration can break the ferromagnetic alignment reducing the overall magnetic moment. Standard magnetic and nonmagnetic molecular systems have been also recently investigated for the occurrence of noncollinear spin states [20,21].

Recent Born-Oppenheimer molecular dynamics investigations on small-sized transition-metal clusters showed that structures belonging to different potential energy surfaces (PES), characterized by the spin multiplicity, could share the same energy window. This means that a particular structure can modify its spin state, provided that the spin-orbit mechanism connecting two PES is operative [22]. In gas phase synthesis, nucleation takes place rapidly, and at finite temperature, a number of possible structures, differing by small cohesion energies can then coexist and eventually modify their magnetic properties.

We have investigated the electronic structure of nickel aggregates up to twelve atoms. The magnetic properties have been computed paying particular attention to the spin polarization of the local magnetic moments. We have also determined the thermal average for structures having different spin multiplicities.

We focus on the possible paths connecting different stable structures belonging to different spin states. These stable structures are close enough in energy to allow for a thermodynamic competition even at low temperatures. We also investigated the nature of the transition states connecting the stable structures.

II. METHODOLOGY

The ground-state structures of nickel clusters have been obtained at different spin multiplicities by searching the minimum in the PES. The local minimum has been confirmed by computing the hessian and performing the corresponding vibrational analysis. The starting structures have been obtained by a random search algorithm sampling using the Gupta model potential [23] parametrized by Cleri and Rosato [24]. The electronic structure has been computed in the DFT framework (GAUSSIAN 09 code [25]) using the Stuttgart-Dresden relativistic pseudopotentials [26] and two different semilocal exchange and correlation functionals, PW91 [27], PBE [28], and a meta-GGA functional M06L [29]. Each converged structure has been tested for the stability of the Kohn-Sham (KS) wave functions following the standard procedure of Bauernschmitt and Ahlrichs [30]. In all cases, we found that the KS one-determinant description suffices to describe the ground state of the investigated nickel clusters. Different energetic descriptors have been computed according to the following standard definitions. The binding energy (BE) is defined by

$$E_b = E(\mathrm{Ni}) - E(\mathrm{Ni}_n)/n, \tag{1}$$

where $E(\mathrm{Ni})$ is the energy in the ground state of one nickel atom and $E(\mathrm{Ni}_n)$ is the energy of the ground state for the Ni_n cluster. The second difference in energy is defined by

$$\Delta^2 E(\mathrm{Ni}_n) = E(\mathrm{Ni}_{n-1}) + E(\mathrm{Ni}_{n+1}) - 2E(\mathrm{Ni}_n), \tag{2}$$

in accordance with the definition that the clusters with $\Delta^2 E(\mathrm{Ni}_n) > 0$ are more stable than those having $\Delta^2 E(\mathrm{Ni}_n) < 0$. The fragmentation energy has been computed by

$$E_{\mathrm{frag}} = E(\mathrm{Ni}_{n-1}) + E(\mathrm{Ni}) - E(\mathrm{Ni}_n). \tag{3}$$

$\Delta^2 E(\mathrm{Ni}_n)$ and E_{frag} were computed and plotted as a function of the cluster size. These results are summarized in Ref. [31].

Noncollinear spin states in nickel clusters introduce small changes in geometries, binding energies, and magnetism in respect to a collinear approach. Although a limitation, we did not include the noncollinear possibility in the determination of the electronic structure of the systems considered in this investigation. The local magnetic moment per atom in the cluster can be estimated by performing the charge population analysis for each spin contribution. The spin polarization yields the population unbalance and the local magnetic moment.

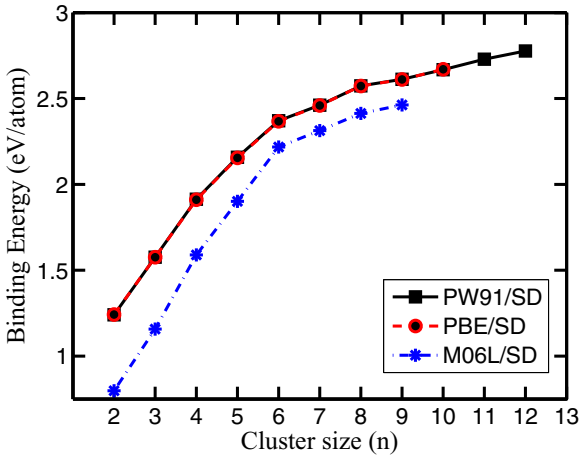

FIG. 1. (Color online) Binding energy for the small-sized nickel clusters at the ground state.

Since some of the clusters exhibit a ground state very close in energy to other spin multiplicities (M), we have carried out a thermal average to compute the average magnetic moment considering a Maxwell-Boltzmann distribution. We have explored the transition state connecting structures close in energy and belonging to two different spin multiplicities. The transition state (TS) connecting two structures was located by using the STQN method implemented by Peng *et al.* [32,33].

III. RESULTS AND DISCUSSION

We present the results of the electronic structure computations on small-sized nickel clusters (Ni_n, $2 \leqslant n \leqslant 12$). In Fig. 1, we plot the computed BE obtained for the nickel clusters. The use of PBE and PW91 pure GGA functionals allows us to obtain systematic results on the same ground. The meta-GGA functional (M06L) is claimed to perform well with transition metals (geometries and overall properties) [34,35]. However, besides the lower BE values found with respect to pure GGA results, the ground state was wrongly obtained (wrong spin multiplicities) for some clusters (see Ref. [31]). This inability to predict the right ground states forces us to disregard this functional. Nevertheless, these results act as boundaries for the binding energies. It should be noted that the nickel dimer is the only cluster for which the BE energy is known (≈1.07 eV/at). Our prediction with GGA functionals overestimates these data, while the meta-GGA computations underestimate it. The M06L density functional systematically underestimates the cohesion energy in weakly bounded systems and it is expected that this trend is also followed in larger systems [34,36].

In Fig. 2, the average magnetic moment is reported for at the PW91/SD level of theory and compared with previous experimental values and some of the theoretical calculations. The local magnetic moment histograms for selected nickel clusters at relevant multiplicities are sketched in Fig. 3. In Tables I–III, we summarize the binding energies for each structure at the different investigated spin multiplicities using the total electronic energy and the free Gibbs energy computed at PW91/SD theory level. The ground-state structures and spin densities are sketched in Fig. 4 for the PW91/SD. The structures reported in Fig. 4 correspond to a spin multiplicity yielding the lowest electronic as well as the formation Gibbs free energies. In Table IV, we summarize the cluster abundance obtained by considering a Maxwell-Boltzmann distribution of nanoparticles at each temperature. Complementary computations were carried out at PBE/SDD theory level. Since our results are consistent with those at PW91/SDD level, they are summarized in Ref. [31].

Ni_2 has been extensively investigated. Experimentally, this dimer exhibits a triplet ground state [37] having an average binding energy of 1.07 eV, bond distance of 2.193 Å, and a normal frequency of 355.45 cm^{-1}. Several electronic structure studies has been carried out on this system [7,38–54]. Mainly based on DFT, these computations are consistent with the triplet ground state, systematically overestimating the binding energy. In the present work, we obtain consistently a triplet ground state with 1.241 eV for the binding energy and 2.11 Å for the bond length (BL).

It remains a subject of controversy whether Ni_3 has the higher D_{3h} symmetry [11,47,54] or if it is the lower C_{2v} symmetry [7,38,40,42–44,46,49,50,53] that represents the ground-state structure. Both symmetries exhibit a triplet state. The BE has been found to be 1.46 [44], 1.58 [49], 1.66 [50], and 1.70 eV [46], to be compared with our result of 1.58 eV (Tables I–III). The local magnetic moments are found to be 0.73, 0.73, and $0.54\mu_B$. These differences are due to the symmetry reduction, which is in good agreement with previous reports [49]. A higher spin state (M = 5) is found only 63 meV above the ground state. The statistical free energy analysis indicates that above room temperature a small contribution appears (0.02% at 400 K).

The ground state of Ni_4 cluster has been found in the quintet spin multiplicity exhibiting a slightly distorted (D_{2d}) tetrahedral geometry [11,39,42–44,46,47,49,50,53,54]. However, Reuse *et al.* predicted a septet state in D_{2d} geometry and a flat square isomer with the same BE. The BE for the ground-state structure scatters from 1.91 to 5.43 eV, depending on the investigation report. We agree with the previous quintet state reports (BE = 1.91 eV) and local magnetic moments between $0.78\mu_B$ and $1.32\mu_B$.

For Ni_5 clusters, two possible structures has been found for the ground state, a quintet spin state with a trigonal bipyramid (D_{3h}) geometry [42,43,46,49,50,53–55] and a septet state with a square pyramid (C_{4v}) geometry [7,39,52,56]. The average magnetic moment for the C_{4v} geometry is reported as $1.2\mu_B$ [7,39,52,56,57], while in the D_{3h} geometry a lower magnetic moment of $0.8\mu_B$ [42,43,46,49,50,53,54] is frequently found. Błonsky *et al.* [11] reported, after scalar relativistic calculations, a quintet state in a D_{3h} symmetry and local magnetic moments between $0.71\mu_B$ and $0.8\mu_B$, which is in good agreement with our results for the trigonal bipyramid (M = 5, Fig. 3). It is important to note that Błonsky *et al.* take into account the spin-orbit coupling and add $\approx 0.09\mu_B$ to each local magnetic moment. Even with this increase in the magnetic moment it does not reach the value predicted by Reuse *et al.* [40], who obtained a trigonal bipyramid D_{3h} with a total magnetic moment of $1.6\mu_B$ in a nonet state, more stable than the square pyramid by 1 eV. To our knowledge, Reuse *et al.* [40] have performed the only DFT

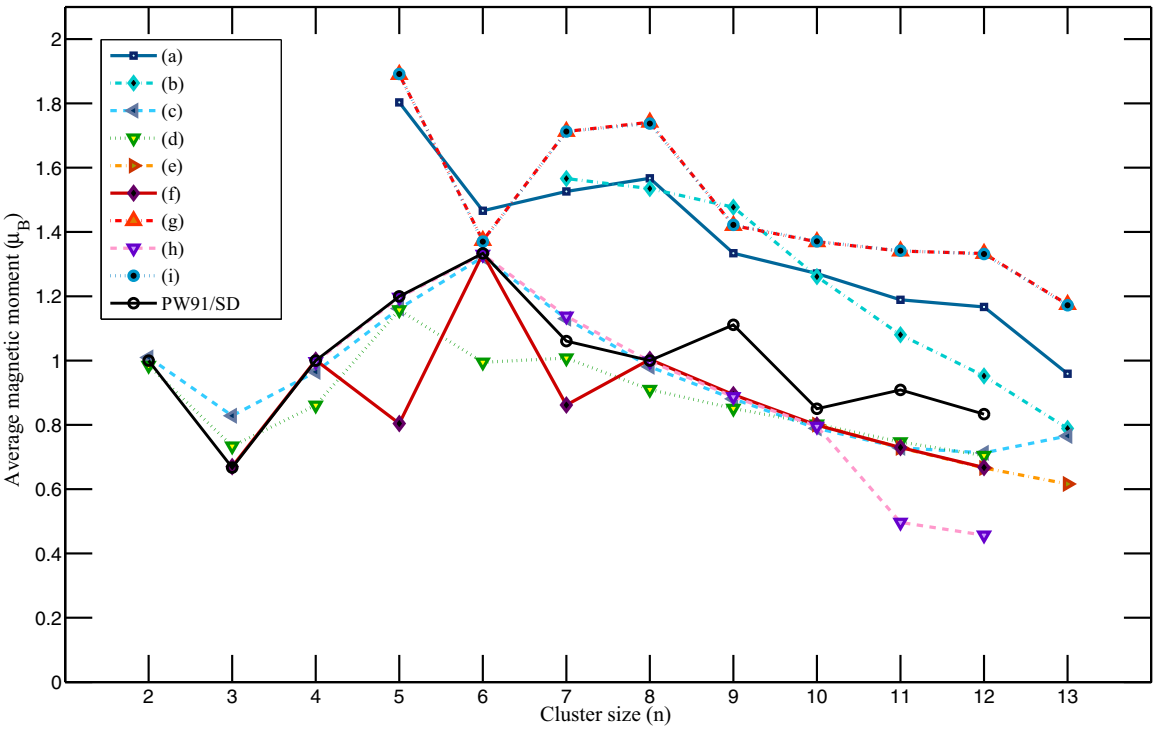

FIG. 2. (Color online) Average magnetic moment per atom for the ground state at the PW91/SD level of theory and magnetic moment per atom from experiment, see Refs. (a) [58], (b) [64], and theory, (c) [7], (d) [52], (e) [65], (f) [54], (g) [57], (h) [56], and (i) [55].

TABLE I. Multiplicities M, magnetic order MO (FI ferrimagnetic, FM ferromagnetic), average nearest-neighbor $\langle d \rangle$ (in Å), dispersion σ (in Å), binding energy BE (in eV/atom), and difference in energy with respect to the ground state ΔBE (in eV/atom) for Ni_n clusters at the PW91/SD level of theory. BE_G and ΔBE_G are the free energy and free energy differences (in eV/atom), respectively.

n	Structure	M	MO	$\langle d \rangle$	σ	BE	ΔBE	BE_G	ΔBE_G
2	Dimer	3	FM	2.11		1.240	0.000	1.103	0.000
		5	FM	2.18		0.603	0.637	0.476	0.627
		7	FM	2.37		−0.898	2.138	−1.016	2.119
3	Triangle	3	FM	2.24	$\theta = 58.51$	1.576	0.000	1.382	0.000
		5	FM	2.18	$\theta = 124.48$	1.513	0.063	1.334	0.048
		7	FM	2.36	$\theta = 60.0$	1.201	0.374	1.023	0.359
4	Tetrahedron	3	FI	2.30	0.07	1.848	0.066	1.599	0.070
		5	FM	2.30	0.06	1.914	0.000	1.669	0.000
		7	FM	2.24	0.02	1.785	0.128	1.551	0.118
5a	Trigonal bipyramid	3	FI	2.34	0.06	2.096	0.062	1.817	0.064
		5	FM	2.32	0.04	2.122	0.036	1.843	0.038
		7	FM	2.33	0.05	2.109	0.049	1.831	0.050
		9	FM	2.34	0.07	2.070	0.088	1.790	0.091
5b	Square pyramid	3	FI	2.30	0.01	2.053	0.105	1.773	0.107
		5	FI	2.30	0.02	2.092	0.066	1.816	0.065
		7	FM	2.30	0.00	2.158	0.000	1.881	0.000
		9	FM	2.30	0.07	2.048	0.110	1.768	0.113
6	Octahedron	3	FI	2.34	0.04	2.261	0.110	1.954	0.117
		5	FI	2.33	0.07	2.283	0.087	1.981	0.090
		7	FI	2.32	0.03	2.293	0.078	1.987	0.084
		9	FM	2.35	0.05	2.371	0.000	2.071	0.000
		11	FM	2.36	0.03	2.051	0.320	1.761	0.311

TABLE II. (cont.) Multiplicities M, magnetic order MO (FI ferrimagnetic, FM ferromagnetic), average nearest-neighbor $\langle d \rangle$ (in Å), dispersion σ (in Å), binding energy BE (in eV/atom), and difference in energy with respect to the ground state ΔBE (in eV/atom) for Ni_n clusters at the PW91/SD level of theory. BE_G and ΔBE_G are the free energy and free energy differences (in eV/atom), respectively.

n	Structure	M	MO	$\langle d \rangle$	σ	BE	ΔBE	BE_G	ΔBE_G
7a	Octahedron	3	FI	2.32	0.05	2.380	0.081	2.063	0.085
	capped	5	FI	2.35	0.05	2.413	0.048	2.095	0.053
		7	FM	2.33	0.05	2.410	0.051	2.096	0.051
		9	FM	2.30	0.03	2.461	0.000	2.148	0.000
		11	FM	2.37	0.04	2.341	0.120	2.024	0.124
7b	Pentagonal	3	FI	2.37	0.05	2.386	0.075	2.064	0.083
	bipyramid	5	FI	2.37	0.04	2.396	0.065	2.078	0.070
		7	FM	2.34	0.03	2.458	0.003	2.146	0.002
		9	FM	2.35	0.05	2.448	0.013	2.133	0.015
8	Octahedron	3	FI	2.35	0.04	2.505	0.068	2.173	0.071
	bicapped	5	FI	2.34	0.05	2.518	0.056	2.187	0.057
		7	FI	2.35	0.05	2.539	0.035	2.206	0.037
		9	FM	2.34	0.04	2.574	0.000	2.244	0.000
		11	FM	2.36	0.04	2.464	0.110	2.136	0.108
9		3	FI	2.32	0.04	2.513	0.099	2.176	0.095
		5	FI	2.35	0.06	2.567	0.045	2.229	0.042
		7	FI	2.35	0.04	2.586	0.026	2.245	0.026
		9	FM	2.33	0.04	2.564	0.048	2.228	0.043
		11	FM	2.35	0.05	2.612	0.000	2.271	0.000
		13	FM	2.35	0.05	2.492	0.120	2.156	0.115
10	Antiprism	3	FI	2.36	0.04	2.651	0.017	2.298	0.021
		5	FI	2.37	0.04	2.647	0.021	2.295	0.024
		7	FI	2.34	0.03	2.643	0.025	2.293	0.026
		9	FM	2.35	0.06	2.668	0.000	2.319	0.000
		11	FM	2.36	0.05	2.665	0.003	2.318	0.001
		13	FM	2.34	0.03	2.619	0.049	2.272	0.047

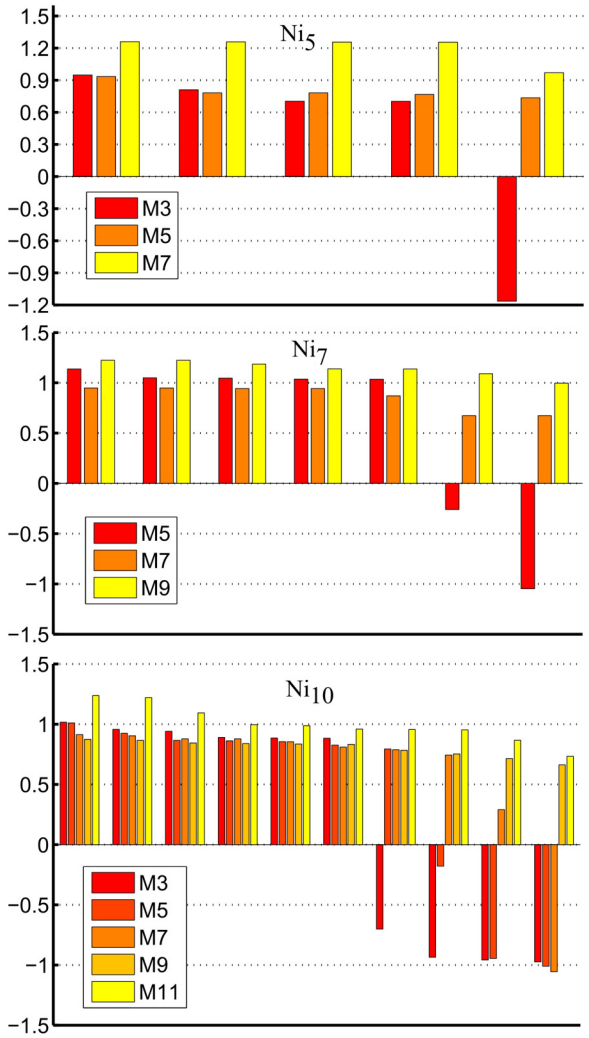

FIG. 3. (Color online) Local magnetic moments in selected nickel clusters.

TABLE III. (cont.) Multiplicities M, magnetic order MO (FI ferrimagnetic, FM ferromagnetic), average nearest-neighbor $\langle d \rangle$ (in Å), dispersion σ (in Å), binding energy BE (in eV/atom), and difference in energy with respect to the ground state ΔBE (in eV/atom) for Ni_n clusters at the PW91/SD level of theory. BE_G and ΔBE_G are the free energy and free energy differences (in eV/atom), respectively.

n	Structure	M	MO	$\langle d \rangle$	σ	BE	ΔBE	BE_G	ΔBE_G
11		3	FI	2.34	0.05	2.689	0.040	2.330	0.043
		5	FI	2.33	0.04	2.684	0.045	2.328	0.045
		7	FI	2.35	0.06	2.695	0.033	2.338	0.034
		9	FM	2.35	0.05	2.715	0.014	2.359	0.014
		11	FM	2.36	0.04	2.729	0.000	2.372	0.000
		13	FM	2.35	0.04	2.691	0.038	2.339	0.033
12		5	FI	2.35	0.04	2.722	0.055	2.359	0.057
		7	FI	2.36	0.03	2.732	0.045	2.370	0.047
		9	FM	2.36	0.04	2.752	0.025	2.393	0.023
		11	FM	2.34	0.04	2.777	0.000	2.416	0.000
		13	FM	2.36	0.04	2.736	0.041	2.378	0.038

calculations that estimated a value for the magnetic moment, close to the experimental value of $1.8\mu_B$ [58]. Parks *et al.* [59] proposed the trigonal bipyramid or the square pyramid as possible structures for Ni_5 via molecular nitrogen adsorption. However, they cannot assert which one of these structures is the most favorable. Owing to the different possible structures and multiplicities, Khanna and Jena [6] investigated via photo detachment spectroscopy the ground-state structure. They reported a square pyramid (C_{4v}, M = 7) as the ground-state geometry and a distorted trigonal bipyramid (M = 5) almost degenerated, only 0.02 eV above the ground state.

Our results on the Ni_5 cluster exhibit a septet ground state in a slightly distorted square pyramid geometry (Fig. 4). However, a M = 5 structure in a trigonal bipyramid geometry is lower in BE by 36 meV. Both structures exhibit a ferromagnetic coupling (Fig. 4). As the square pyramid structure can be easily viewed as a distorted trigonal bipyramid [6], and due to the previous discrepancies, we investigated the possible transition states connecting each two structures that are close in free energy.

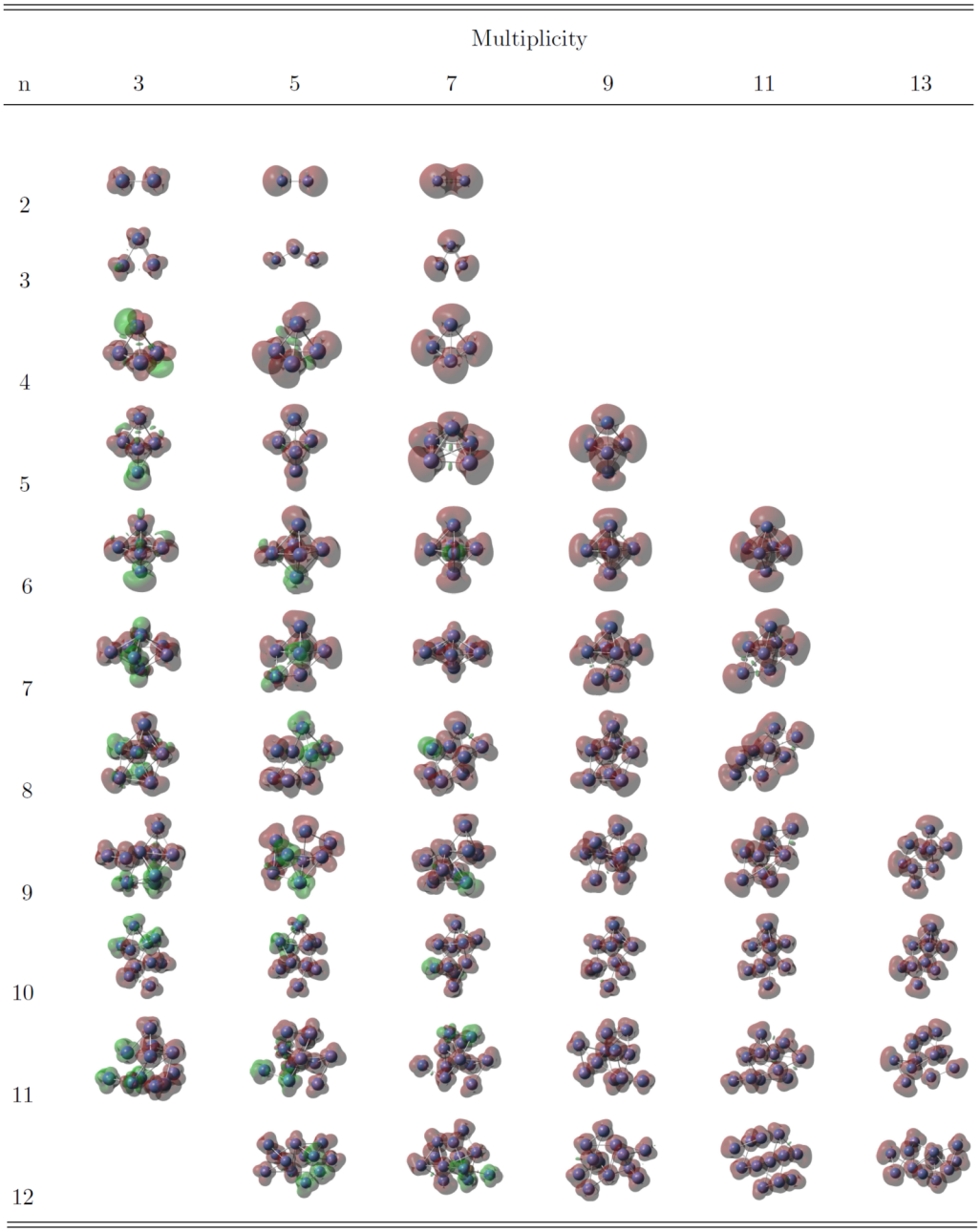

FIG. 4. (Color online) Spin densities for $Ni_n (2 \leqslant n \leqslant 12)$ at the PW91/SD level of theory.

Here, a small digression is necessary about the possible mechanisms connecting two PES belonging to different spin multiplicities. In standard photophysical processes, two possible mechanisms for nonradiative transitions are commonly considered: *internal conversion* involving a vibrational coupling mechanism and an *intersystem crossing* (IC) allowing a change in the spin multiplicity through a spin-orbit (SO) coupling mechanism. The probability of an IC transition is proportional to the SO matrix elements connecting the n-electron wave functions of the initial and final states belonging each to a different spin multiplicity. This computation necessitates a particular SO (relativistic) Hamiltonian approximation. The SO matrix elements have been investigated and codes are only available for singlet-triplet transitions [60–63].

We start with the ground-state septet displayed with the ■ symbol in Fig. 5. The possible transition states are sketched in this figure and described in what follows. The TS connecting the septet square pyramid (7■) and the septet trigonal bipyramid (7▲) structures, belonging to the same PES, is observed ≈0.042 eV above the local minimum 7▲. The 7▲ bond lengths between the apical atoms and among the atoms forming the central triangle are ≈0.02 Å larger than the bond lengths forming the square in the 7■ structure. The TS shows ferromagnetic coupling suggesting that the transition from 7▲ to 7■ requires only the shortening of the bond lengths. The local magnetic moment of 7▲ structure, which is lower in the apical atoms ($1.19\mu_B$) and higher in two of the atoms in the triangle ($1.35\mu_B$), becomes homogeneous in the 7■

TABLE IV. Thermal average composition for Ni_n clusters. The abundance for the clusters n(M) = 2(3),3(3), 4(5),6(9),8(9),9(11),11(11),12(11), where n is the number of nickel atoms and M is the ground-state ($T = 0$ K) multiplicity, which is 100%. These results were obtained by considering a Maxwell-Boltzmann distribution using the Gibbs free energies. In parenthesis, we include the abundance obtained by using the total electronic energy. Data obtained at PW91/SD theory level.

n	Structure	M	400 K	293.15 K	135.5 K
5	SP	3	0 (0)	0 (0)	0 (0)
		5	0.01 (0.01)	0 (0)	0(0)
		7	99.52 (99.35)	99.94 (99.91)	100 (100)
	TBP	3	0.01 (0.01)	0 (0)	0 (0)
		5	0.39 (0.55)	0.05 (0.08)	0(0)
		7	0.07 (0.08)	0.01 (0.01)	0 (0)
7	OC	5	0 (0)	0 (0)	0 (0)
		7	0 (0)	0 (0)	0(0)
		9	58.61 (62.39)	63.31 (69.31)	77.63 (86.88)
	PBP	5	0 (0)	0 (0)	0 (0)
		7	38.45 (32.85)	35.62 (28.81)	22.36(13.08)
		9	2.94 (4.76)	1.07 (2.06)	0.01 (0.04)
10		3	0.14 (0.54)	0(0.10)	0 (0)
		5	0.05 (0.15)	0 (0.02)	0 (0)
		7	0.03 (0.05)	0(0)	0 (0)
		9	57.22 (68.27)	59.95 (74.51)	70.56 (91.14)
		11	42.56 (30.99)	40.03 (25.37)	29.44 (8.86)

structure ($1.26\mu_B$), just conserving one atom with a lower local magnetic moment ($0.97\mu_B$, Fig. 3). As it can be appreciated in the energy profile plot, the transition from the ground state 7■ to the 7▲ state requires a larger amount of energy (≈0.25 eV) making this less probable.

The TS over the same PES M = 5, between the quintet square pyramid (5■) and the quintet trigonal bipyramid (5▲) is =100 meV above the 5■ (Fig 5, right side)—both structures show ferromagnetic coupling (Fig. 4). For the 5■ structure, the distortion is more evident, however, the bond lengths in the square are essentially equal (2.29 Å). The transition to the 5▲ structure (Fig. 5, left side) increases the bond lengths between the apical atoms and the atoms in the central triangle: 2.33 and 2.35 Å with respect to each apical atom. This indicates that the gain in free energy results in a more open structure. The local magnetic moments in the 5■ structure are more scattered ($0.47\sim1.1\mu_B$) than those in the 5▲ structure ($0.77\sim0.93\mu_B$, Fig. 3), as a result of a higher stability, the local magnetic moments achieve homogeneity. In the other case, even the difference between the local minimum 5▲ and 5■ is ≈0.134 eV, to reach the TS from 5▲ requires 234 meV making this an unlikely transition.

Another possible transition can be considered between the quintet trigonal bipyramid (5▲) and the 7■ structure. The local minimum 5▲ seems to suggest that a transition to the higher spin multiplicity 7■ could be done directly via the TS M = 5 through the SO mechanism (≈0.183 eV). The lower coordination and shortening in the bond lengths from 5▲ to 7■ results in the enhancement of the local magnetic moments (Fig. 3). The TS M = 5 shows a ferromagnetic coupling. The TS M = 7 (Fig. 5) from the 7■ to the 5▲ is highly unlikely due to the large amount of free energy required to achieve it (≈0.707 eV), besides the loss of symmetry and the increase of the bond lengths.

Moreover, based on the local minimum of the 5▲ structure, two more transition states can be found in addition to those already mentioned above. One is directed towards the 7▲ structure and the other towards the triplet trigonal bipyramid (3▲) structure. The TS M = 5 from 5▲ to 7▲, which is ≈0.242 eV above in free energy, requires a greater difference in the bonding distances between the apical atoms and the central triangle (2.29∼2.37 Å). The TS M = 7 from the 7▲ structure to the 5▲ structure is energetically equivalent (≈41 meV) to the TS 7▲ to 7■, which allows for a possible transition to the lowest spin state only due to SO mechanism. The case

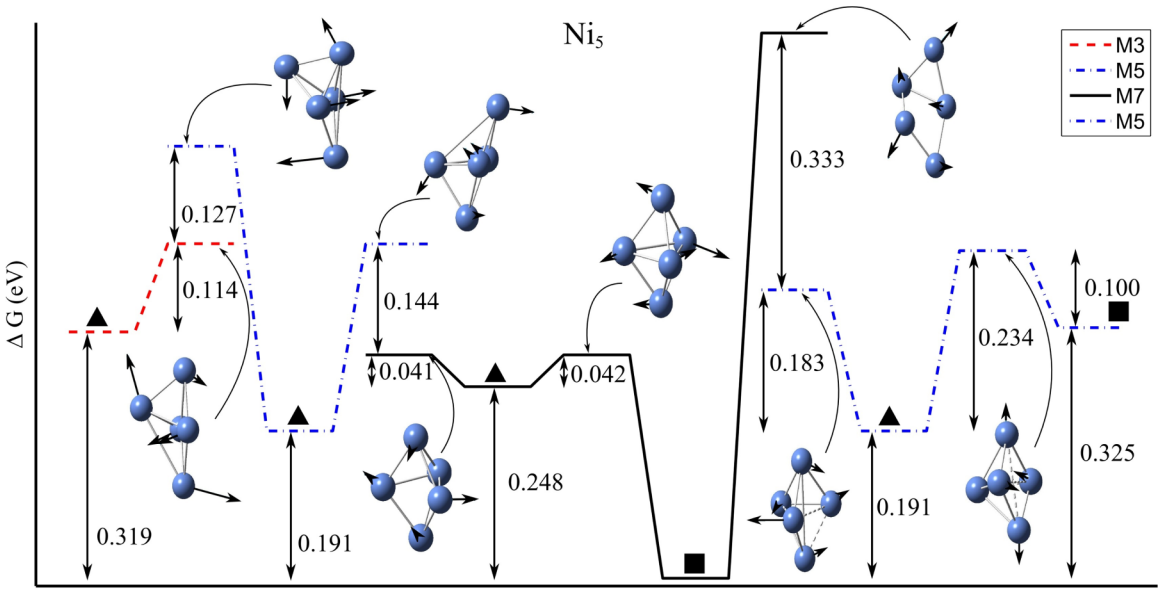

FIG. 5. (Color online) Free energy profiles connecting two spin multiplicities ground-state structures for selected nickel clusters. The square pyramid geometry is represented by ■ and the trigonal bipyramid is represented by ▲.

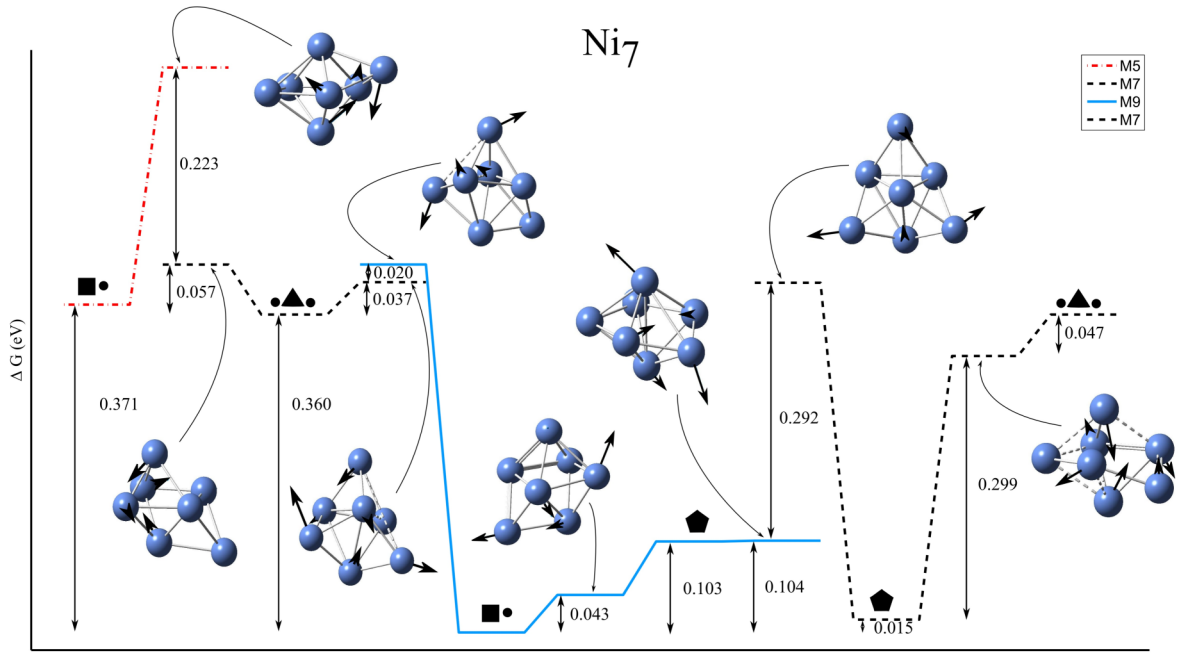

FIG. 6. (Color online) Free energy profiles connecting two spin multiplicities ground-state structures for selected nickel clusters.

of the TS M = 5 from the 5▲ to the 3▲ structure requires ≈0.369 eV. In addition, a loss of homogeneity of the local magnetic moments indicating a ferrimagnetic coupling was observed in the TS. The transition from the 3▲ structure needs ≈0.114 eV to reach the local minimum 7▲ preserving the same geometry but with a spin density rearrangement from ferrimagnetic to ferromagnetic coupling (see Fig. 3).

Ni_6 is found close to octahedral geometry, consistent with previous theoretical [7,11,43,49,52,54–56] and experimental results [59]. We found M = 9 for the ground state in good agreement with previous results [7,11,49]. We found that any other isomer appears high in energy marginally contributing to the overall composition at all temperatures.

For Ni_7, a capped octahedron geometry in the M = 9 spin state has been found [8,9,43,46,49]. In this work, the ground state for the Ni_7 structure is found in the capped octahedron geometry with M = 9 multiplicity (Fig. 4). However, a pentagonal bipyramid with M = 7 multiplicity is found lower in BE by 3 meV (Tables I–III) in agreement with previous results [8,9]. In Table IV, the abundance of Ni_7 clusters at different temperatures indicates a possible competition among different structures and multiplicities.

The TS connecting the M = 9 capped octahedron (9 ■●) and the M = 9 pentagonal bipyramid (9⬠) structures, which are close in free energy (Fig. 6), is ≈43 meV above the ground state 9■●. The TS structure is close in geometry to the 9■● structure, which indicates that the gain in energy from the 9⬠ structure to the 9■● structure is due to the shortening of the bond lengths between the atoms in the octahedron and the rearrangement of the local magnetic moments from the 9⬠ ($1.05\sim1.30\mu_B$) to the 9■● structure ($1.00\sim1.22\mu_B$, Fig. 3) conserving the ferromagnetic coupling. Another possible transition in the same PES is from the 9⬠ structure to the septet pentagonal bipyramid structure (7⬠). This TS seems to be equivalent to the previous TS mentioned because it is 1 meV above the local minimum 9⬠. The SO coupling mechanism can be responsible for reaching a lower multiplicity state while preserving the geometry by just increasing the bond lengths between the atoms in the pentagon and decreasing the bond lengths between the apical atoms and the atoms in the pentagon, to reach both homogeneous bond lengths (2.34 Å, Tables I–III) and homogeneous local magnetic moments ($0.87\sim0.95\mu_B$, Fig. 3) leaving only the apical atoms with a lower magnetic moment ($0.67\mu_B$). On the other hand, the TS from the 9■● structure to the M = 7 bicapped trigonal bipyramid (7 ● ▲●) is very unlikely due to the great amount of required energy (≈417 meV).

The TS from the 7 ● ▲● to the 7⬠ structure (right side in Fig. 6) is possible in the same PES by gaining energy from the 7 ● ▲● structure (≈47 meV) to reach the TS by forming a more open central structure close to the 7⬠ geometry. The average bond lengths for both structures are almost the same (Tables I–III), but the local magnetic moments rearrange from the 7 ● ▲● ($0.72\sim0.92\mu_B$) to the 7⬠ structure ($0.87\sim0.95\mu_B$) as was previously mentioned. An FM coupling is observed in both structures. In the same PES, the TS from the 7⬠ structure to a higher spin state (M = 9) is highly improbable due to the free energy required (≈396 meV) and the SO mechanism.

Two possible TS are observed in the same M = 7 PES (left side Fig. 6) starting from the 7 ● ▲● structure. The first reaches a higher spin state (M = 9), which is ≈37 meV above the local minimum. A greater local magnetic moment homogeneity is observed in the 9⬠ structure (Fig. 3), allowing the transition due to the SO coupling mechanism to reach the ground state. The second TS is observed to go to the M = 5 capped octahedron 5■● structure (≈57 meV). This TS can be less probable because it requires, due to SO mechanism, to go from the FM coupling to the FI coupling in the structure and elongation of the bond lengths.

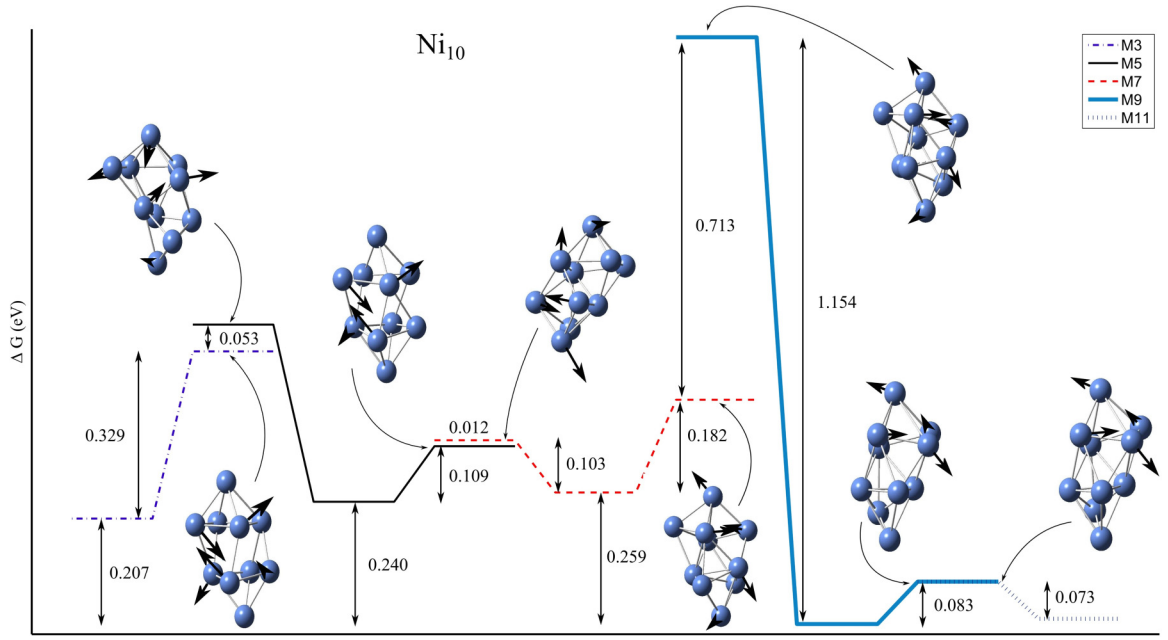

FIG. 7. (Color online) Free energy profiles connecting two spin multiplicities ground-state structures for selected nickel clusters.

The last TS observed is the one from the 5■● structure to a higher spin state (M = 7). The TS is ≈280 meV above the local minimum, which makes this TS unlikely.

The population analysis of these isomers close in BE yields a contribution of 86.88% for the 9■● structure and 13.08% for the 7⬠ structure at 135.5 K; the contributions computed by using the free energy are similar (77.63% and 22.36%, respectively). At room temperature (293.15 K) the 9■● contribution decreases (69.31% and 63.31% for the electronic and free energies respectively), the 7⬠ contribution increases (28.81% and 35.62% for the electronic and free energies, respectively), and a new contribution appears for the 9⬠ structure (2.06% and 1.07% for the electronic and free energies, respectively). At a higher temperature (400 K), the decrease of the 9■● contribution is more evident (62.39% and 58.61% for the electronic and free energies, respectively), and the increase for the 7⬠ (32.85% and 38.45% for the electronic and free energies, respectively) and the contribution for the 9⬠ become more evident as well (4.76% and 2.94% for the electronic and free energies, respectively).

For Ni_8, different closely related geometries have been reported for the ground state: a 4,4 capped trigonal prism [43], a bisdisphenoid D_{2d} [7,49], and a T_d symmetry [46]. Our results are consistent with a bisdisphenoid geometry in a M = 9 ground state.

For Ni_9, Curotto *et al.* [43] suggested the lowest minimum structure to be a twin trigonal antiprism, a fragment of an hcp crystal. Futschek *et al.* [49] found a capped C_{1h} structure in the M = 9 spin state. A tricapped triangular prism is reported by Lu *et al.* [7] and Song [52] in the M = 9 spin state. However, we found a well defined ground state in the M = 11 multiplicity with a shared octahedron and trigonal bipyramid geometry.

The Ni_{10} cluster exhibits an interesting competition among several different close in geometry structures having different spin multiplicities. The abundance analysis for the Ni_{10} clusters (Table IV) indicates a competition between the M = 9 and 11 associated structures. The contributions for the lower spin state (M = 3∼7) are not statistically significant because are less than 0.5%. The ground state is found to be a 4,4 capped square antiprism, as in previous results [43,49] (double pyramid), in a M = 9 spin state. A second structure (M = 11) is almost degenerate by BE = 3 meV bellow the ground state. The TS energy profile (Fig. 7) clearly indicates that the double pyramid (M = 9) structure is the more stable structure and a transition to a high multiplicity (M = 11) structure is possible since the energy barrier to reach the TS at M = 9 or M = 11 is low (≈83 meV). The local magnetic moments in the ground state (M = 9) are more homogeneous (0.66∼0.84μ_B) than in the M = 11 structure (0.73∼1.24μ_B, Fig. 3) making the M = 9 structure more likely. On the other hand, a complex manifold of structures appears for low spin multiplicities (M = 3∼7). The energy barrier separating the ground-state structure to the M = 7 structure is high (≈1.154 eV) making this transformation very unlikely. However, an M = 7 structure can more easily evolve into the ground state since the energy barrier is around 0.182 eV, arranging the local magnetic moments from FI coupling to FM coupling, almost preserving the BL. Another possible TS from the M = 7 structure is to a lower in BE and spin state structure (4 meV, M = 5, respectively), the TS is 103 meV above the local minimum M = 7; this transition requires the SO coupling mechanism to decrease the spin state, preserving the FI coupling and increasing the BL ≈3 Å. On the other hand, the equivalent TS from M = 5 to that local minimum M = 7 mentioned (≈109 meV) requires arranging the local magnetic moments to a mostly homogeneous order due to the SO coupling mechanism. The other possible TS in the M = 5 PES is to a lower spin state M = 3 (≈349 meV), which is highly unlikely. Finally, the TS from the M = 3 state to a higher M = 5 state requires 329 meV to be reached.

Ni_{11} appears to be in a distorted capped trigonal prism [43,49], a tetra capped pentagonal bipyramid [52], and a

trilayered structure with 3-5-3 stacking [7]. Our results indicate that the ground state has an M = 11 multiplicity in a tricapped antitwin trigonal bipyramid geometry.

Ni_{12} appears in a capped square antiprism structure [43] like Ni_{10}, an incomplete icosahedron [49] in a M = 9 ground state, and a trilayered structure with 3-6-3 stacking [7]. However, we found a well-defined M = 11 ground state in a bicapped antitwin octahedron geometry.

IV. CONCLUSIONS

The present work reports the structural, magnetic properties, and transition states for several structures of Ni_n ($2 \leqslant n \leqslant 12$) that are close to each other energetically. The Ni_{3-8} clusters exhibit slight distortions with respect to the high symmetric geometries. However, Ni_{9-12} clusters show structures that are difficult to assign to a high symmetric form. As the second difference energy indicates, Ni_2, Ni_6, and Ni_8 are the more stable structures. This result is in good agreement with previous reports. The computed magnetic moment compares well with previous theoretical studies. The average magnetic moment is also in good agreement with the experimental results, exhibiting differences that can be either attributed to the accuracy of calculations or the orbital angular momentum contribution.

The spin density analysis shows that the Ni_n ($4 \leqslant n$) clusters exhibit ferrimagnetic coupling at the low spin states reaching a ferromagnetic coupling for higher spin states. The Ni_2 and Ni_3 clusters are ferromagnetic for all the spin states.

The Ni_5 ground state exhibits differences in geometry with respect to the neighboring local minima. The thermal average analysis shows that the Ni_5 clusters are completely dominated by the square pyramid in the septet state. This is clearly observed in the free energy profile. The transition to different geometries in the same or a different potential energy surface is highly improbable.

Ni_7 shows differences in the local minima structures belonging to different potential energy surfaces. The ground state and the nearest local minimum exhibit a competition in the thermal average computation. The Ni_7 cluster is mostly dominated by the octahedron capped structure in the nonet spin state. At room temperature and above, a small contribution appears for the pentagonal bipyramid structure in the nonet state and the contribution for the pentagonal bipyramid in the septet spin state becomes more significant. The free energy profile shows that a transition between the almost energy-degenerated structures is unlikely.

For the Ni_{10} cluster, a competition between two almost energy-degenerated structures is observed in the thermal average computation. Both structures have essentially the same geometry and the contribution for the total composition is mostly dominated by the nonet at lower temperatures. The M = 11 spin state structure becomes more evident as the temperature is increased, reaching almost the same participation at higher temperatures for both spin state structures. The energy profile shows that the transition state between both structures is indistinguishable from a local minimum, due to the spin-orbit coupling mechanism being responsible for reaching a lower or a higher spin state.

ACKNOWLEDGMENTS

The authors would like to thank DGTIC-UNAM for providing to us part of the computational facilities and the financial support provided by DGAPA-UNAM under contract Grant Number: IN112413.

[1] F. Alonso, P. Riente, and M. Yus, Acc. Chem. Res. **44**, 379 (2011).
[2] O. Metin, V. Mazumder, S. Ozkar, and S. Sun, J. Am. Chem. Soc. **132**, 1468 (2010).
[3] A. W. Pelzer, J. Jellinek, and K. A. Jackson, J. Phys. Chem. A **117**, 10407 (2013).
[4] X. He, W. Zhong, C.-T. Au, and Y. Du, Nanoscale Res. Lett. **8**, 446 (2013).
[5] A.-H. Lu, E. e. Salabas, and F. Schüth, Angew. Chem., Int. Ed. **46**, 1222 (2007).
[6] S. N. Khanna and P. Jena, Chem. Phys. Lett. **336**, 467 (2001).
[7] Q. L. Lu, Q. Q. Luo, L. L. Chen, and J. G. Wan, Eur. Phys. J. D **61**, 389 (2011).
[8] N. Desmarais, C. Jamorski, F. A. Reuse, and S. N. Khanna, Chem. Phys. Lett. **294**, 480 (1998).
[9] S. K. Nayak, B. Reddy, B. K. Rao, S. Khanna, and P. Jena, Chem. Phys. Lett. **253**, 390 (1996).
[10] S. N. Khanna, M. Beltran, and P. Jena, Phys. Rev. B **64**, 235419 (2001).
[11] P. Blonski and J. Hafner, J. Phys.: Condens. Matter **23**, 136001 (2011).
[12] T. Oda, A. Pasquarello, and R. Car, Phys. Rev. Lett. **80**, 3622 (1998).
[13] N. Fujima and T. Oda, Eur. Phys. J. D **24**, 89 (2003).
[14] P. Ruiz-Díaz, J. Dorantes-Davila, and G. Pastor, Eur. Phys. J. D **52**, 175 (2009).
[15] C. Köhler, T. Frauenheim, B. Hourahine, G. Seifert, and M. Sternberg, J. Phys. Chem. A **111**, 5622 (2007).
[16] G. Scalmani and M. J. Frisch, J. Chem. Theory Comp. **8**, 2193 (2012).
[17] C. Kohl and G. F. Bertsch, Phys. Rev. B **60**, 4205 (1999).
[18] D. Gatteschi, EPJ Web of Conferences **75**, 05004 (2014).
[19] G. Yao, S. Huang, M. T. Berry, P. S. May, and D. S. Kilin, Mol. Phys. **112**, 546 (2014).
[20] S. Luo and D. G. Truhlar, J. Chem. Theory Comp. **9**, 5349 (2013).
[21] X. Xu, K. R. Yang, and D. G. Truhlar, J. Chem. Theory Comp. **10**, 2070 (2014).
[22] A. M. Köster, P. Calaminici, E. Orgaz, D. R. Roy, J. U. Reveles, and S. N. Khanna, J. Am. Chem. Soc. **133**, 12192 (2011).
[23] R. P. Gupta, Phys. Rev. B **23**, 6265 (1981).
[24] F. Cleri and V. Rosato, Phys. Rev. B **48**, 22 (1993).
[25] M. J. Frisch *et al.*, GAUSSIAN 09 Revision D.01 (Gaussian Inc. Wallingford CT, 2009).

[26] A. Bergner, M. Dolg, W. Küchle, H. Stoll, and H. Preuß, Mol. Phys. **80**, 1431 (1993).
[27] J. Perdew, Phys. Rev. B **45**, 244 (1991).
[28] J. P. Perdew, K. Burke, and M. Ernzerhof, Phys. Rev. Lett. **77**, 3865 (1996).
[29] Y. Zhao and D. G. Truhlar, Theor. Chem. Acc. **120**, 215 (2008).
[30] R. Bauernschmitt and R. Ahlrichs, J. Chem. Phys. **104**, 9047 (1996).
[31] See Supplemental Material at http://link.aps.org/supplemental/10.1103/PhysRevB.91.075428 for details of the BE, $\Delta^2 E$, E_{frag}, and average magnetic moment for PW91/SD, PBE/SD, and M06L/SD; also the spin multiplicities, magnetic order, structural details, and spin densities obtained at the PBE/SD theory level.
[32] C. Peng, P. Y. Ayala, H. B. Schlegel, and M. J. Frisch, J. Comp. Chem. **17**, 49 (1996).
[33] C. Peng and H. Bernhard Schlegel, Isr. J. Chem. **33**, 449 (1993).
[34] N. Marom, A. Tkatchenko, M. Rossi, V. V. Gobre, O. Hod, M. Scheffler, and L. Kronik, J. Chem. Theory Comput. **7**, 3944 (2011).
[35] Y. Minenkov, Å. Singstad, G. Occhipinti, and V. R. Jensen, Dalton Trans. **41**, 5526 (2012).
[36] T. Bučko, S. Lebègue, J. Hafner, and J. G. Ángyán, Phys. Rev. B **87**, 064110 (2013).
[37] J. C. Pinegar, J. D. Langenberg, C. A. Arrington, E. M. Spain, and M. D. Morse, J. Chem. Phys. **102**, 666 (1995).
[38] M. Tomonari, H. Tatewaki, and T. Nakamura, J. Chem. Phys. **85**, 2875 (1986).
[39] P. Mlynarski and D. R. Salahub, J. Chem. Phys. **95**, 6050 (1991).
[40] F. Reuse and S. Khana, Chem. Phys. Lett. **234**, 77 (1995).
[41] N. N. Lathiotakis, A. N. Andriotis, M. Menon, and J. Connolly, J. Chem. Phys. **104**, 992 (1996).
[42] M. Castro, C. Jamorski, and D. R. Salahub, Chem. Phys. Lett. **271**, 133 (1997).
[43] E. Curotto, A. Matro, D. L. Freeman, and J. D. Doll, J. Chem. Phys. **108**, 729 (1998).
[44] B. Chen, A. W. C. Jr, and S. N. Khanna, Chem. Phys. Lett. **304**, 423 (1999).
[45] M. Calleja, C. Rey, M. M. G. Alemany, L. J. Gallego, P. Ordejón, D. Sánchez-Portal, E. Artacho, and J. M. Soler, Phys. Rev. B **60**, 2020 (1999).
[46] M. C. Michelini, R. Pis Diez, and A. H. Juber, Int. J. Quantum Chem. **85**, 22 (2001).
[47] B. Chen, A. Castleman Jr., C. Ashman, and S. N. Khanna, Int. J. Mass Spectrom. **220**, 171 (2002).
[48] V. G. Grigoryan and M. Springborg, Phys. Rev. B **70**, 205415 (2004).
[49] T. Futschek, J. Hafner, and M. Marsman, J. Phys.: Condens. Matter **18**, 9703 (2006).
[50] G. López Arvizu and P. Calaminici, J. Chem. Phys. **126**, 194102 (2007).
[51] I. Onal, A. Sayar, A. Uzun, and S. Ozkar, J. Comp. Theor. Nanoscience **6**, 867 (2009).
[52] W. Song, W.-C. Lu, C. Wang, and K. Ho, Comp. Theor. Chem. **978**, 41 (2011).
[53] S. Goel and A. E. Masunov, J. Mol. Model. **18**, 783 (2011).
[54] B. Reddy, S. Nayak, S. Khanna, B. Rao, and P. Jena, J. Phys. Chem. A **102**, 1748 (1998).
[55] S. Bouarab, A. Vega, M. J. López, M. P. Iñiguez, and J. A. Alonso, Phys. Rev. B **55**, 13279 (1997).
[56] J. Guevara, F. Parisi, A. M. Llois, and M. Weissmann, Phys. Rev. B **55**, 13283 (1997).
[57] F. Aguilera-Granja, S. Bouarab, M. J. López, A. Vega, J. M. Montejano-Carrizales, M. P. Iñiguez, and J. Alonso, Phys. Rev. B **57**, 12469 (1998).
[58] S. E. Apsel, J. W. Emmert, J. Deng, and L. A. Bloomfield, Phys. Rev. Lett. **76**, 1441 (1996).
[59] E. K. Parks, L. Zhu, J. Ho, and S. J. Riley, J. Chem. Phys. **100**, 7206 (1994).
[60] S. Koseki, M. W. Schmidt, and M. S. Gordon, J. Phys. Chem. **96**, 10768 (1992).
[61] S. Koseki, M. S. Gordon, M. W. Schmidt, and N. Matsunaga, J. Phys. Chem. **99**, 12764 (1995).
[62] N. Matsunaga and S. Koseki, Rev. Comp. Chem. **20**, 101 (2004).
[63] S. Chiodo and N. Russo, J. Comp. Chem. **29**, 912 (2008).
[64] M. B. Knickelbein, J. Chem. Phys. **116**, 9703 (2002).
[65] Y. Yao, X. Gu, M. Ji, X. Gong, and D.-s. Wang, Phys. Lett. A **360**, 629 (2007).